Wave Spectrum and Breaking Wave Statistics of Growing and Mature Seas

Tetsu Hara[(1)] and Tobias Kukulka[(2)]

[(1)] Graduate School of Oceanography, University of Rhode Island, USA (thara@uri.edu)

[(2)] Woods Hole Oceanographic Institution, USA

1. Introduction

Accurate predictions of the spectrum and breaking statistics of ocean surface waves are important to both ocean engineers and ocean-atmosphere scientists. For engineers these are key input information for modelling interactions between ocean surface waves and marine structures, as well as modelling a variety of near shore processes driven by surface waves. For oceanographers and meteorologists, understanding surface wave processes is important because they control air-sea exchange of energy, momentum, heat, and gas, and they produce bubbles and sea sprays.

Existing numerical wave models are capable of predicting the surface wave spectrum near the spectral peak. However, they cannot predict the spectrum at higher frequencies (away from the spectral peak) nor the statistics of breaking waves. The objective of this study is to develop a theoretical model framework to predict both the spectrum and the breaking statistics over a broad range of frequencies (wave scales).

2. Coupled model of wind and waves

Since ocean surface waves are forced by wind, and the wind field itself is modified by the presence of surface waves, a coupled model of surface waves and near surface wind is required. By balancing air-side momentum and energy and by conserving wave energy, coupled nonlinear advance–delay differential equations are derived, which govern simultaneously the wave and wind field. The system of equations is closed by introducing a relation between the wave height spectrum and wave dissipation due to breaking.

The wave field is described statistically by the two dimensional wavenumber spectrum $\Psi(k,\theta)$, or alternatively the saturation spectrum, $B(k,\theta) = k^4\Psi(k,\theta)$, and the two-dimensional distribution of breaking waves, $\Lambda(k,\theta)$. The average breaking crest length of waves, at wavenumber *k* and propagating in the direction θ relative to the wind, is given by $\Lambda(k,\theta)kdkd\theta$ (Phillips 1985).

a. Air-side momentum conservation

Within the constant stress layer, the total wind stress τ_0 partitions into turbulent Reynolds stress τ_t, and wave-induced parts. The wave-induced stress is decomposed further into one part due to the form drag of nonbreaking waves, τ_w, and another part due to the form drag of breaking waves, τ_b. The breaking stress transfers momentum directly into the wave so that it effectively reduces the momentum transport through the air inside the wave boundary layer. The total momentum budget can be written as

$$\tau_0 = \tau_t(z) + \tau_w(z) + \tau_b(z) = const.$$

Following Makin and Kudryavtsev (1999), the wave-induced momentum flux τ_w at height *z* into nonbreaking waves is given by integrating the product of the wave spectrum and the momentum input rate, truncated at the inner layer height (Belcher and Hunt 1993). The

form drag of breaking waves τ_b at height *z* is parameterized by integrating the product of the breaking distribution function and the momentum input rate, truncated at the height of the breaking crest, following Kudryavtsev and Makin (2001) and Kukulka et al. (2007).

b. Air-side energy conservation

The total energy equation can be obtained by considering the mean energy budgets of mean, wave-induced, and turbulent motions (Hara and Belcher 2004). The mean air-side energy equation, including the wave effect, can be written as

$$\frac{d[u(\tau_t + \tau_w]}{dz} - \varepsilon(z) - \frac{d\Pi_w}{dz} - e_b(z) = 0,$$

where Π_w denotes the energy flux induced by nonbreaking waves and e_b is the rate of air energy transferred to breaking waves. The former is parameterized by integrating the spectral energy flux $I_w(k,\theta)$ after Hara and Belcher (2004). The latter is obtained from the spectral energy flux to breaking waves $I_b(k,\theta)$, following Kukulka et al. (2007).

c. Wave energy conservation

The energy input rate due to wind forcing is balanced by the wave dissipation rate, *D*, and nonlinear interactions, *NL*,

$$I_w(k,\theta) + I_b(k,\theta) + NL(k,\theta) - D(k,\theta) = 0.$$

Following Phillips (1985), we set *NL* to be proportional to the cube of $B(k,\theta)$, and *D* to be proportional to $\Lambda(k,\theta)$.

d. Relation between Λ and B

To solve the above equations for *B*, Λ, τ_t, and *u*, one must prescribe a functional relationship between $\Lambda(k,\theta)$ and $B(k,\theta)$. We set

$$\Lambda(k,\theta) \propto k^{-1}(B(k,\theta))^3\left[1+\left(\frac{B(k,\theta)}{B_{sat}}\right)^n\right]$$

where $n >> 1$. The first term of the sum is based on the argument that there is a wavenumber range in which nonlinear interactions and dissipation are proportional to each other (Phillips 1985). The second term of the sum is based on the observation that Λ increases rapidly for $B > B_{sat}$, where B_{sat} is the "threshold saturation level" (Alves and Banner 2003).

3. Results and discussion

The model is first applied to strongly wind forced conditions (young seas) with frequent wave breaking, where the contribution of nonbreaking waves is negligible (Kukulka et al. 2007). Figure 1 illustrates how the wave field (breaking statistics) develops according to our theory for a fixed total wind stress. For very young seas the breaking statistics is the largest at the lowest wavenumber (spectral peak). As the wave field develops, the number of breaking waves at the peak rapidly decreases. When the spatial sheltering effect (air flow separation behind breaking crests) is included, the result remains qualitatively similar.

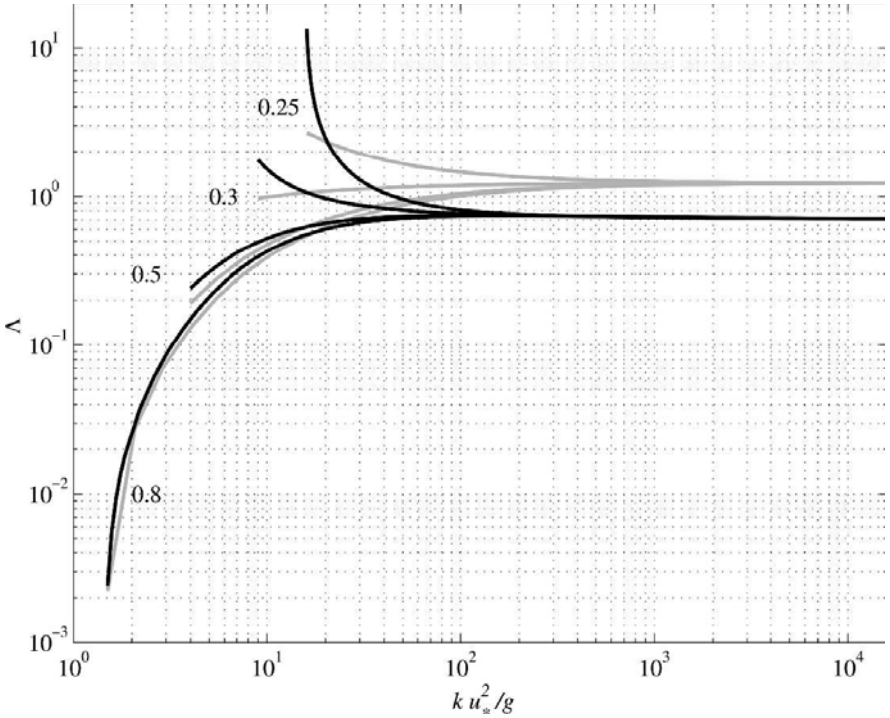

Figure 1. Breaking-wave distribution for wave age $c_p / u_* = 0.25$, 0.3, 0.5, and 0.8, where c_p is the phase speed at the spectral peak and u_* is the air friction velocity. Grey and black lines are solutions with and without spatial sheltering effect, respectively.

Next, the model is applied to growing and mature seas including the contribution of nonbreaking waves (Kukulka and Hara, 2008a, b). The results of the saturation spectrum and the breaking statistics are shown in Figure 2. The saturation spectrum B converges quickly to B_{sat} except near the spectral peak of developed seas. For the two more developed cases, the distribution of breaking waves at low wavenumbers coincides with the nonbreaking solution (gray dashed line), indicating the dominance of wind input to nonbreaking waves. As the wavenumber increases, solutions first converge to the breaking-only solution (gray solid line) and then to the breaking-dominant asymptotic solution (parallel straight gray lines). Therefore, the breaking wave effect is more pronounced for shorter, strongly forced (young) wind waves.

4. Conclusion

We have developed a coupled wind and wave model. The conservation of air-side momentum and energy, as well as wave energy, leads to a coupled system of nonlinear advance–delay differential equations for the wave height spectrum, the breaking wave distribution, and the two air-side profiles of wind speed and turbulent stress. The system of equations is closed by introducing a relation between the breaking wave distribution and the wave height curvature spectrum such that above a threshold of *B*, the number of breaking waves rapidly increases.

The input to breaking waves continuously increases with inverse wave age until the input to the spectral peak is dominated by breaking waves. The major wind input to shorter waves away from the spectral peak is determined by breaking waves even for developed seas. In summary, the effect of breaking waves plays a significant role and needs to be incorporated so as to model coupled wind and wave dynamics more realistically.

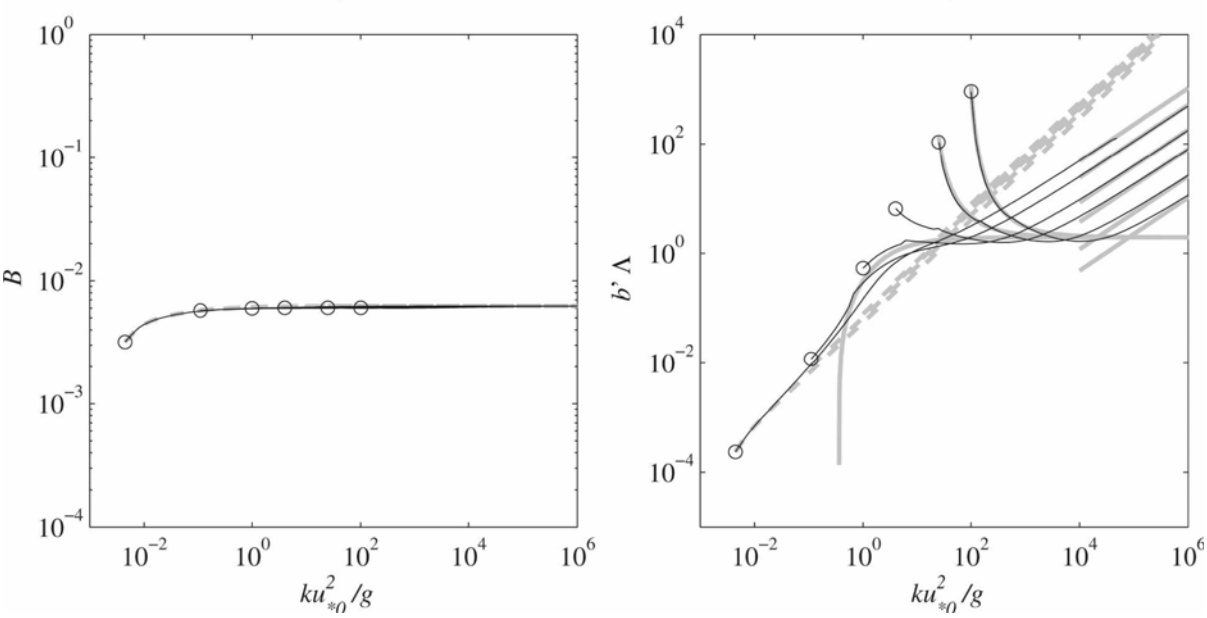

Figure 2. Numeric solutions (black lines) of saturation spectrum (left) and breaking statistics (right) at wave ages 15, 3.0, 1.0, 0.5, 0.2, and 0.1, indicated by circles from left to right. Solution without input to breaking waves (gray dashed line), solution with only input to breaking waves (gray solid line), and asymptotic solutions at high wavenumbers (parallel straight gray lines).

References

Alves, J. H. G. M., and M. L. Banner, 2003: Performance of a saturation-based dissipation-rate source term in modeling the fetch-limited evolution of wind waves. J. Phys. Oceanogr., 33, 1274–1298.

Belcher, S. E., and J. C. R. Hunt, 1993: Turbulent shear flow over slowly moving waves. J. Fluid Mech., 251, 109–148.

Hara, T., and S. E. Belcher, 2002: Wind forcing in the equilibrium range of wind-wave spectra. J. Fluid Mech., 470, 223–245.

Kudryavtsev, V. N., and V. K. Makin, 2001: The impact of air-flow separation on the drag of the sea surface. Bound.-Layer Meteor., 98, 155–171.

Kukulka, T., and H. Hara, 2008: The effect of breaking waves on a coupled model of wind and ocean surface waves. Part I: Mature seas. J. Phys. Oceanogr., 38, 2145–2163.

Kukulka, T., and H. Hara, 2008: The effect of breaking waves on a coupled model of wind and ocean surface waves. Part II. Growing seas. J. Phys. Oceanogr., 38, 2164–2184.

Kukulka, T., T. Hara, and S. Belcher, 2007: A model of the air–sea momentum flux and breaking-wave distribution for strongly forced wind waves. J. Phys. Oceanogr., 37, 1811–1828.

Makin, V. K. and V. N. Kudryavtsev, 1999: Coupled sea surface-atmosphere model. 1. Wind over waves coupling. J. Geophys. Res., 104 (C4), 7613–7624.

Phillips, O., 1985: Spectral and statistical properties of the equilibrium range in wind-generated gravity waves. J. Fluid Mech., 156, 505–531.